Identification of the First Specific Inhibitor of p90 Ribosomal S6 Kinase (RSK) Reveals an Unexpected Role for RSK in Cancer Cell Proliferation

Jeffrey A. Smith,[1,2] Celeste E. Poteet-Smith,[1] Yaming Xu,[3] Timothy M. Errington,[1] Sidney M. Hecht,[3] and Deborah A. Lannigan[1,4]

[1]Center for Cell Signaling, Departments of [2]Pathology and [3]Chemistry, and [4]Microbiology, University of Virginia, Charlottesville, Virginia

Abstract

p90 ribosomal S6 kinase (RSK) is an important downstream effector of mitogen-activated protein kinase, but its biological functions are not well understood. We have now identified the first small-molecule, RSK-specific inhibitor, which we isolated from the tropical plant *Forsteronia refracta*. We have named this novel inhibitor SL0101. SL0101 shows remarkable specificity for RSK. The major determinant of SL0101-binding specificity is the unique ATP-interacting sequence in the amino-terminal kinase domain of RSK. SL0101 inhibits proliferation of the human breast cancer cell line MCF-7, producing a cell cycle block in G_1 phase with an efficacy paralleling its ability to inhibit RSK in intact cells. RNA interference of RSK expression confirmed that RSK regulates MCF-7 proliferation. Interestingly, SL0101 does not alter proliferation of a normal human breast cell line MCF-10A, although SL0101 inhibits RSK in these cells. We show that RSK is overexpressed in ~50% of human breast cancer tissue samples, suggesting that regulation of RSK has been compromised. Thus, we show that RSK has an unexpected role in proliferation of transformed cells and may be a useful new target for chemotherapeutic agents. SL0101 will provide a powerful new tool to dissect the molecular functions of RSK in cancer cells. (Cancer Res 2005; 65(3): 1027-34)

Introduction

The p90 ribosomal S6 kinase (RSK) family are serine/threonine protein kinases that are downstream effectors of mitogen-activated protein kinase (MAPK). In humans, four isoforms have been identified, each the product of distinct genes. The RSK isoforms have similar overall structure with two nonidentical kinase domains separated by a linker region of ~100 amino acids and short amino- and carboxyl-terminal segments. The amino-terminal kinase domain (NTKD) is most closely related to p70 S6 kinase (p70 S6K), whereas the carboxyl-terminal kinase domain (CTKD) is most similar to the calmodulin-dependent protein kinases (1). The regulation of RSK is extremely complex and seems to require a cascade of phosphorylations that result from the action of MAPK, the CTKD of RSK, and 3-phosphoinositide-dependent protein kinase-1 (2–6). RSK contains a docking site for MAPK at its extreme carboxyl terminus, and this docking site is a requirement for specific MAPK phosphorylation of RSK (7, 8). The NTKD is responsible for phosphorylating exogenous substrates and preferentially phosphorylates at serine/threonine residues that lie in RXRXXS/T or RRXS/T motifs (9). The only known function for the CTKD is autophosphorylation of the linker region.

The mechanism of RSK activation has been the subject of many studies, but little progress has been made in understanding the biological functions of RSK. The few substrates identified for RSK include transcription factors like estrogen receptor-α, cyclic AMP response element-binding protein (CREB), c-Fos, and IκBα/nuclear factor-κB (10–14) as well as other kinases, such as glycogen synthase kinase-3, the p34cdc2-inhibitory kinase Myt1, and recently the mitotic checkpoint kinase Bub1 (15–17). The paucity of data concerning key biological roles of RSK in somatic cells results primarily from the difficulty in distinguishing RSK function from those of MAPK itself and of the many other downstream MAPK effectors. This difficulty has arisen because of the lack of RSK-specific inhibitors.

We endeavored to identify a RSK-specific inhibitor by screening botanical extracts using high-throughput screening assays. We have an extensive collection of botanical extracts derived from plants of rare genera. This unique library was collected as part of the original collaboration between the National Cancer Institute and the Department of Agriculture initiated in 1960 for the systematic collection of plants. Herein we describe the discovery, identification, and characterization of the only known small molecule that specifically inhibits RSK *in vitro* and *in vivo*. The inhibitor, which we have named SL0101, was used to uncover a novel and unexpected link between RSK activity and transformed cell proliferation.

Materials and Methods

Kinase Assays. Glutathione *S*-transferase fusion protein (1 μg) containing the sequence RRRLASTNDKG (for serine/threonine kinase assays) or VSVSETDDYAEIIDEEDTFT (for tyrosine kinase assays) was adsorbed in the wells of LumiNunc 96-well polystyrene plates (MaxiSorp surface treatment). The wells were blocked with sterile 3% tryptone in PBS and stored at 4°C for up to 6 months. Kinase (5 nmol/L) in 70 μL of kinase buffer [5 mmol/L -glycerophosphate (pH 7.4), 25 mmol/L HEPES (pH 7.4), 1.5 mmol/L DTT, 30 mmol/L $MgCl_2$, 0.15 mol/L NaCl] was dispensed into each well. Compound at indicated concentrations or vehicle was added, and reactions were initiated by the addition of 30 μL ATP for a final ATP concentration of 10 μmol/L unless indicated otherwise. Reactions were terminated after 10 to 45 minutes by addition of 75 μL 500 mmol/L EDTA (pH 7.5). All assays measured the initial velocity of reaction. After extensive washing of wells, anti-phospho-p140 antibody, a polyclonal phosphospecific antibody developed against the phosphopeptide, CGLA(pS)TND, and horseradish peroxidase (HRP)–conjugated anti-rabbit antibody (211-035-109, Jackson ImmunoResearch Laboratories, West Grove, PA) were used to detect serine phosphorylation of the substrate. Specificity of the

Note: Supplementary data for this article are available at Cancer Research Online (http://cancerres.aacrjournals.org/).

Requests for reprints: Jeffrey A. Smith, Center for Cell Signaling, University of Virginia Health Science Center, Box 800577, Hospital West, 7041 Multistory Building, Charlottesville, VA 22908-0577. Phone: 434-924-1152; Fax: 434-924-1236; E-mail: jas8j@virginia.edu.

anti-phospho-p140 for detection of the phosphorylated peptide is shown in the signal-to-background ratio of the high-throughput screening assays as well as the immunoblots presented in Fig. 5*B* and Supplemental Fig. 3. HRP-conjugated anti-phosphotyrosine antibody (RC20, BD Transduction Laboratories, San Diego, CA) was used for phosphotyrosine detection. HRP activity was measured using Western Lightning Chemiluminescence Reagent (NEL102, Perkin-Elmer Life Sciences, Boston, MA) according to the manufacturer's protocol. Maximum and minimum activity is the relative luminescence detected in the presence of vehicle and 200 mmol/L EDTA, respectively. His-tagged active RSK and focal adhesion kinase (FAK) were expressed in Sf9 cells and purified using NiNTA resin (Qiagen, Valencia, CA). Baculovirus was prepared using the Bac-to-Bac baculovirus expression system (Invitrogen, Carlsbad, CA). Protein kinase A (PKA) was bacterially expressed and activated as described (18). Active MAPK/stress-activated protein kinase-1 (MSK1) and p70 S6K were purchased from Upstate Biotechnology (Charlottesville, VA). Immunoprecipitation and kinase assays were done as described previously (6) using the immobilized GST fusion proteins and ELISA as above.

Cell Culture. For proliferation studies cells were seeded at 2500 to 5000 cells per well in 96 well tissue culture plates in the appropriate medium as described by American Type Culture Collection (Manassas, VA). After 24 hours, the medium was replaced with medium containing compound or vehicle as indicated. Cell viability was measured at indicated time points using CellTiter-Glo assay reagent (Promega, Madison, WI) according to the manufacturer's protocol. For *in vivo* inhibition studies, cells were seeded at 2.5×10^5 cells per well in 12-well cell culture clusters. After 24 hours, the cells were serum starved for 24 hours and then incubated with compound or vehicle for 3 hours before a 30-minute phorbol dibutyrate (PDB) stimulation or a 30-minute stimulation of a cocktail containing 500 nmol/L insulin, 150 ng/mL epidermal growth factor, and 5% FCS (I-E-F). Cells were lysed as described previously (12). The lysates were normalized for total protein, electrophoresed, and immunoblotted. Antibodies used on cell lysates include anti-pan-MAPK (610124) and anti-Ran (610341) from BD Transduction Laboratories; anti-phospho-MAPK (V8031) from Promega; anti-phospho-Akt motif (9611), anti-phospho-CREB (9191), anti-phospho-PKA motif (9621), anti-phospho-protein kinase C (PKC) motif (2261), anti-phospho-S6 (2211), and anti-phosphotyrosine (9411) from Cell Signaling Technology (Beverly, MA); anti-phospho-p140 generated against the phosphopeptide for the HRP-ELISA; and anti-RSK1 (C-21) and anti-RSK2 (E-1) from Santa Cruz Biotechnology (Santa Cruz, CA).

Cell Cycle Analysis. MCF-7 cells were seeded at a density of 1.5×10^5 in 35-mm tissue culture plates and treated the next day for 24 hours with either ethanol, 100 μmol/L SL0101, or 25 μmol/L U0126. Single-cell suspensions were collected, and pellets were fixed in ice-cold ethanol (70%) for 2 hours. After centrifugation of the samples, propidium iodide (50 μg/mL) and RNase (20 units/mL) were added to the pellets for 15 minutes at 37°C. Samples were analyzed by flow cytometry.

Gene Silencing. siGENOME SMARTpool short interfering RNA (siRNA) oligonucleotides to RSK1 (RPS6KA1) and RSK2 (RPS6KA3) mRNA and the siCONTROL nontargeting siRNA 1 (Dharmacon Research, Inc., Lafayette, CO) were used for the gene silencing studies. Briefly, MCF-7 cells were grown to ~70% confluence and trypsinized. The cells were resuspended at a density of 1×10^6 cells/mL into 2 mL antibiotic-free DMEM containing 10% FCS in a sterile 50 mL tube. Oligonucleotides (200 pmol) were resuspended following the manufacturer's protocols and diluted in 250 μL DMEM and in a separate tube 10 μL LipofectAMINE 2000 was diluted in 250 μL DMEM. The diluted siRNA and diluted LipofectAMINE 2000 were then combined, gently mixed, and allowed to incubate for 20 minutes at room temperature. The siRNA-LipofectAMINE 2000 mixture was added directly to the cells. The cells were centrifuged 4 hours after transfection and resuspended in DMEM containing 10% FCS and antibiotics. The resuspended cells were seeded into 96-well tissue culture plates for proliferation assays and 6-well tissue clusters for determining expression levels. Cells were incubated for 48 hours before initiation of cell viability measurement. The cells for determining expression levels were harvested 72 hours after plating.

Breast Tissue Analysis. These studies complied with the University of Virginia institutional review board and federal requirements. Pathologic specimens were obtained in such a manner that subjects cannot be identified directly or through identifiers linked to the subjects. Frozen human breast tissue samples were examined by frozen section, and areas of cancers were excised from the frozen blocks. Samples of normal and benign breast tissue were obtained from frozen blocks containing abundant epithelium. The tissue was finely ground using mortar and pestle under liquid nitrogen. Ground tissue was added to heated 2× SDS loading buffer and boiled for 3 minutes. Protein concentration of the lysates was measured, and lysates were electrophoresed on SDS-PAGE, immunoblotted, and normalized using anti-Ran antibody. The normalized samples were then electrophoresed and immunoblotted with anti-RSK1, anti-RSK2, and anti-active MAPK antibodies. The intensity of the enhanced chemiluminescence was determined by densitometry and confirmed that data obtained were in the linear range. Each gel contained a sample that permitted normalization between immunoblots. Normal (12 samples) and cancer type (48 samples; lobular and ductal carcinoma) were recorded by the pathology laboratory.

Results and Discussion

Identification of the RSK-Specific Inhibition. High-through put screening ELISAs that produces luminescence as a measure of substrate phosphorylation were developed to identify RSK inhibitors from botanical extracts. The Z' factor of an assay is a statistical characteristic of the quality of the assay with respect to the dynamic range and data variation of the signal measurements (19). A Z' factor of 1 represents the ideal assay with no background and no deviation of signal, whereas a $Z' \leq 0.5$ indicates that the signal window is small to nonexistent. The Z' of the HRP-ELISA developed is ~0.7, indicating a sufficient dynamic range for identifying modulators of kinase activity (Fig. 1*A*). To validate the assay, we determined the IC_{50} of the ATP mimetic H89 for PKA and the IC_{50} of the nonspecific PKC inhibitor Ro 318220 for RSK2, PKA, p70 S6K, and MSK1. The values were consistent with published reports (Fig. 1*B*), which show that the HRP-ELISA we developed is suitable for identifying kinase inhibitors.

Botanical extracts were screened for the presence of a RSK-specific inhibitor. To discriminate extracts containing serine/threonine kinase inhibitors from those containing nuisance compounds, a dual screen of the extracts was done using either a constitutively active RSK2 isoform (RSK2) or the catalytic domain of the tyrosine kinase FAK. One extract that inhibited RSK2 without inhibiting FAK is from *Forsteronia refracta*, a member of the Apocynaceae (dogbane) family found in the South American rainforest (Fig. 2*A*). To determine whether the *F. refracta* extract contained a general serine/threonine kinase inhibitor, activities of the archetypal serine/threonine kinase PKA and of two kinases most closely related to RSK2, p70 S6K and MSK1, were measured in the presence of varying amounts of extract (Fig. 2*B*). Amounts of extract that inhibited RSK2 activity by 90% did not inhibit PKA, p70 S6K, or MSK1 to a greater extent than FAK. Thus, the *F. refracta* extract contains an inhibitor with specificity for RSK2 relative to these other AGC kinase family members.

Fractionation of the extract led to isolation of an active component with an *in vitro* IC_{50} of 89 nmol/L in the presence of 10 μmol/L ATP, the K_m of ATP for RSK (Fig. 3*A* and *B*). Structural determination identified the inhibitor, which we have termed

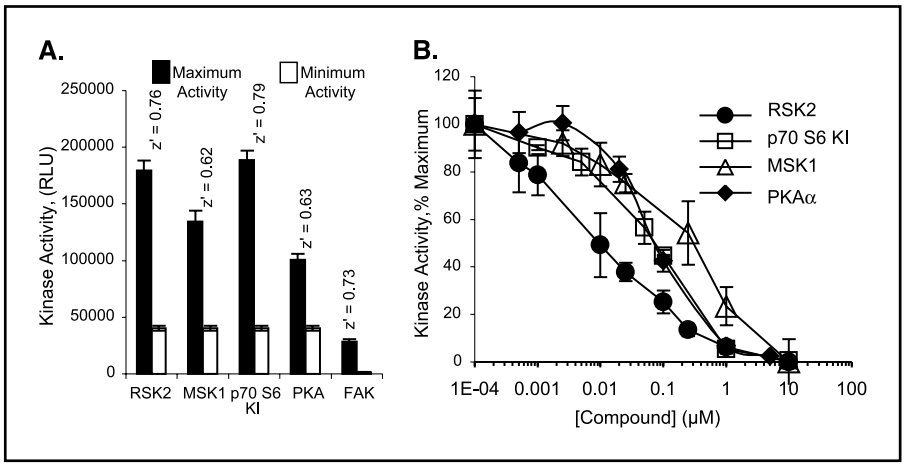

Figure 1. Characterization of the HRP-ELISA. *A,* determination of *Z'* for the HRP-ELISA. Kinase assays were done using immobilized substrate. Reactions were initiated by the addition of 10 μmol/L ATP (final concentration). Reactions were terminated after 10 to 45 minutes. All assays measured the initial reaction velocity. Extent of phosphorylation was determined using phosphospecific antibodies directly labeled with HRP-conjugated or phosphospecific antibodies in combination with HRP-conjugated secondary antibodies. HRP activity was measured as described in Materials and Methods. Maximum and minimum activity is the relative luminescence detected in the presence of vehicle and 200 mmol/L EDTA, respectively. *Columns,* mean (n = 3 in triplicate); *bars,* SD. *B,* inhibition curves generated with the HRP-ELISA. Assays were done as described in *A*. Maximum activity was measured in the presence of vehicle. Inhibition of RSK2, p70 S6K, and MSK1 catalytic activity by Ro 318220 (IC_{50} = 10, 60, and 180 nmol/L, respectively) and inhibition of PKA catalytic activity by H89 (IC_{50} = 60 nmol/L). Kinase activity measured in the presence of the varying concentrations of compound is presented as the percentage of maximum activity. *Points,* mean (n = 2 in triplicate); *bars,* SD.

SL0101, as a kaempferol glycoside (Fig. 3*B*; Supplemental Table 1; ref. 20). The IC_{50} of kaempferol, the flavonoid constituent of SL0101, was determined to be 15 μmol/L for RSK (Fig. 3*A*). Therefore, the rhamnose moiety of SL0101 increases the affinity for RSK by >150-fold. Purified SL0101 is specific for inhibition of RSK activity compared with that of p70 S6K and MSK1 (Fig. 3*C*). SL0101 did not influence the ability of RSK to achieve maximal velocity but altered the K_m of ATP for RSK and is therefore competitive with respect to ATP with a dissociation constant, K_i, of 1 μmol/L (Fig. 3*D*).

SL0101 Interacts with the NTKD of RSK. RSK contains two nonrelated kinase domains in a single polypeptide chain. As stated above, the regulation of RSK is extremely complex and requires activity of both kinase domains. Therefore, inhibition of RSK by SL0101 could occur through interaction with either the NTKD or the CTKD. To determine the domain inhibited by SL0101, we compared the ability of SL0101 to decrease the activity of wild-type or a truncation mutant of RSK2 containing only the NTKD [RSK2(1-389)] (Fig. 4*A*). SL0101 effectively inhibited the isolated RSK2 NTKD.

Because SL0101 is an ATP competitor, we compared the ATP-binding pockets of the AGC kinase family members to identify the determinants of SL0101 specificity. Alignment of the residues forming the ATP-binding pocket of RSK with that of p70 S6K, MSK1, and PKA revealed a difference in the primary structure of the linker region between the two lobes of the catalytic core that contacts the adenosine of ATP (Fig. 4*B*). BLAST analysis indicates that the sequence ^{145}LILDFLRGGDLFT^{157}, the adenosine-interacting loop (AIL), is unique to members of the RSK family. Molecular modeling of residues forming the AIL of the RSK NTKD is shown in Fig. 4*C*. Comparing the AIL models of the RSK NTKD with that of p70 S6K revealed a difference in the dimensions of the pocket created by the AIL. To examine the importance of this region in determining SL0101 specificity, a mutant RSK2 was created in which the p70 S6K-AIL (^{147}LILEYLSGGELFM^{159}) replaced that of RSK2 (RSK2-AILmutant). The RSK2-AILmutant is an active kinase that was inhibited by Ro 318220 to the same extent as was wild-type RSK2; however, SL0101 was much less effective in inhibiting the mutant in comparison with wild-type RSK2 or wild-type RSK1 (Fig. 4*D*). Therefore, the unique AIL of the RSK NTKD is a major determinant for SL0101 specificity. Taken together, these results indicate that inhibition of RSK by

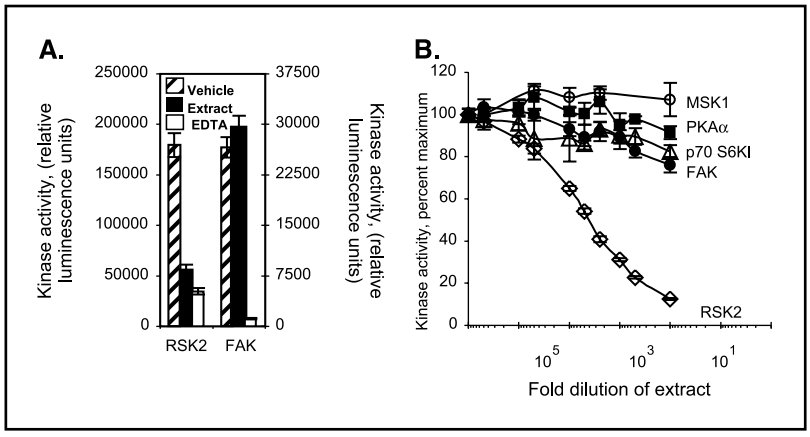

Figure 2. Characterization of the *F. refracta* extract. *A,* effect of the extract on RSK and FAK catalytic activity. Assays were done as described in Fig. 1*A*. Maximum activity was measured in the presence of vehicle. Kinase activity measured in the presence of the extract is presented as the percentage of maximum activity. *Columns,* mean (n = 2 in triplicate); *bars,* SD. *B,* the extract is specific for inhibition of RSK activity. Assays were done as described in Fig. 1*A*. Maximum activity was measured in the presence of vehicle. The nonspecific inhibitor H89 was used as a positive control (data not shown). *Points,* mean (n = 2 in triplicate); *bars,* SD.

SL0101 occurs through competition with ATP for the nucleotide-binding site of the NTKD and further attests to the specificity of SL0101.

SL0101 Is an Effective RSK Inhibitor in Intact Cells. To determine whether SL0101 inhibits RSK in intact cells, phosphorylation of p140, a RSK substrate of unknown function (6), was examined in a human breast cancer cell line MCF-7. Preincubation of cells with 100 μmol/L SL0101 abrogated PDB-induced p140 phosphorylation as did 50 μmol/L U0126, a MAPK/extracellular signal-regulated kinase (ERK) kinase inhibitor (Fig. 5*A*). SL0101 did not affect the phosphorylation of RSK2, as indicated by the reduced electrophoretic mobility of RSK2, nor the activation of MAPK, as detected by the anti-active MAPK antibody (Fig. 5*A*). Therefore, SL0101 does not inhibit upstream kinases necessary for PDB-stimulated RSK activation (i.e., MAPK, MAPK/ERK kinase, Raf, and PKC). These data indicate that SL0101 is membrane permeable and is effective in intact cells. We have shown previously that p140 phosphorylation is not observed in cells treated with the MAPK/ERK kinase inhibitor PD98059. However, p140 phosphorylation does occur in PD98059-treated cells expressing constitutively active RSK2 (6). Thus, p140 is downstream of RSK. To determine whether RSK2 can directly phosphorylate p140, lysates from serum-starved MCF-7 cells treated with vehicle, SL0101, or U0126 and stimulated with PDB or vehicle were transferred to nitrocellulose. The nitrocellulose was incubated in the presence or absence of purified, active, recombinant RSK2 and then immunoblotted. As seen in Fig. 5*B*, RSK can directly phosphorylate immobilized p140. Thus, RSK activity is sufficient for phosphorylation of p140 in intact cells (6) and p140 is phosphorylated by RSK *in vitro*. Taken together, these results suggest that p140 phosphorylation can be used to directly detect RSK activity in intact cells. Additionally, the levels of p140 phosphorylation detected after *in vitro* incubation with active RSK are similar whether the cells were treated with vehicle, SL0101, or U0126. Therefore, the decreased levels of phosphorylated p140 observed in cells treated with SL0101 or U0126 result from reduction of p140 phosphorylation and not alteration of the protein levels. Thus, SL0101 is an effective and specific RSK inhibitor in intact cells.

SL0101 Inhibits Proliferation of MCF-7 Cells. The importance of MAPK to proliferation and oncogenesis is well established (21). However, the role that RSK plays in these processes has not been examined. Therefore, we determined whether SL0101 could inhibit the growth of the human breast cancer cell line MCF-7. Remarkably, SL0101 inhibited proliferation of the MCF-7 line with an efficacy paralleling its ability to inhibit RSK in intact cells but had no effect on the growth of the normal breast cell line MCF-10A (Fig. 6*A* and *B*). Therefore, although SL0101 inhibits RSK activity in MCF-10A cells (Fig. 5*A*), it does not inhibit their growth. Removal of SL0101 after 72 hours resulted in growth of the MCF-7 cells (Fig. 6*C*). Thus, SL0101 is not toxic and preferentially inhibits the growth of the breast cancer cell line relative to that of the normal breast cell line.

Consistent with its antiproliferative effects on cell growth, SL0101 produced a block in the G_1 phase of the cell cycle in MCF-7 cells (Fig. 6*D*). The percentage of cells in G_1 was 38% for vehicle-treated control cells and increased to 67% in SL0101-treated cells with a concomitant decrease in the percentage of cells in both G_2-M

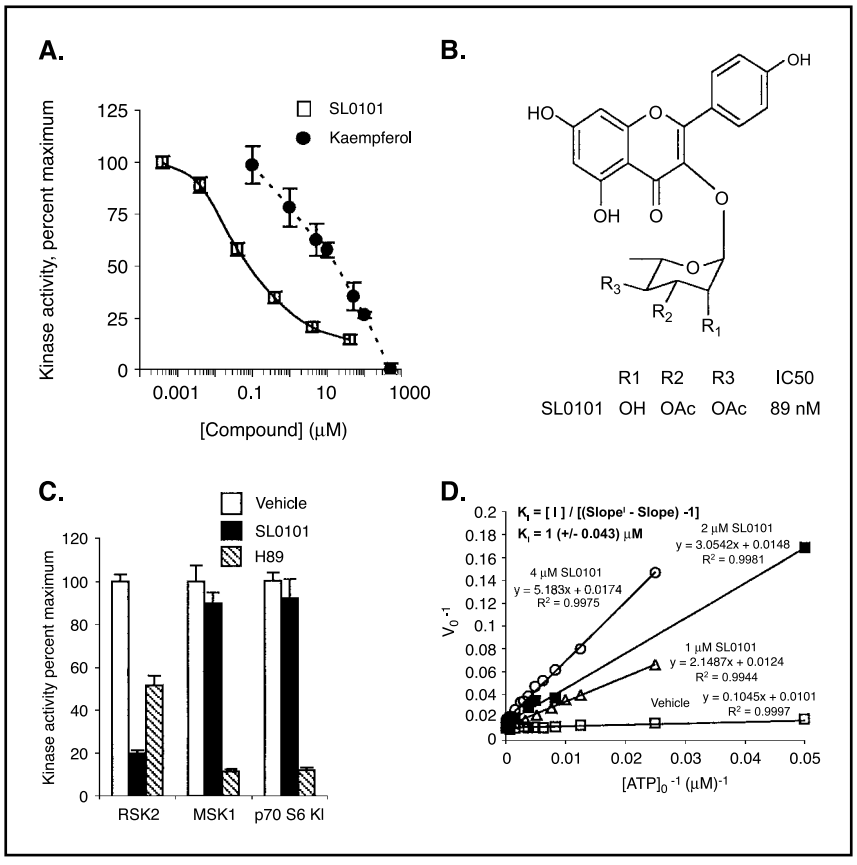

Figure 3. Characterization of SL0101. *A,* inhibition curves of SL0101 and Kaempferol. Potency of purified SL0101 and kaempferol in inhibiting RSK catalytic activity was measured in assays as described in Fig. 1*A*. *Points,* mean (n = 2 in triplicate); *bars,* SD. *B,* structure of SL0101. *C,* SL0101 is specific for inhibition of RSK activity. Kinase assays were done as described in Fig. 1*A* in the presence of vehicle, 2 μmol/L SL0101, or 10 μmol/L H89. *Columns,* mean (n = 3 in triplicate); *bars,* SD. *D,* K_i of SL0101 for RSK2. The inhibitory constant (K_i) of SL0101 for RSK2 was determined by measuring the kinase activity, as described in Fig. 1*A*, in the presence of a constant concentration of SL0101 (1, 2, or 4 μmol/L) and increasing concentrations of ATP. The slope of the plot is increased by the factor $[1 + ([I] / K_i)]$. Thus, the dissociation constant of the enzyme-inhibitor complex was determined to be ~1 μmol/L (n = 2 in triplicate).

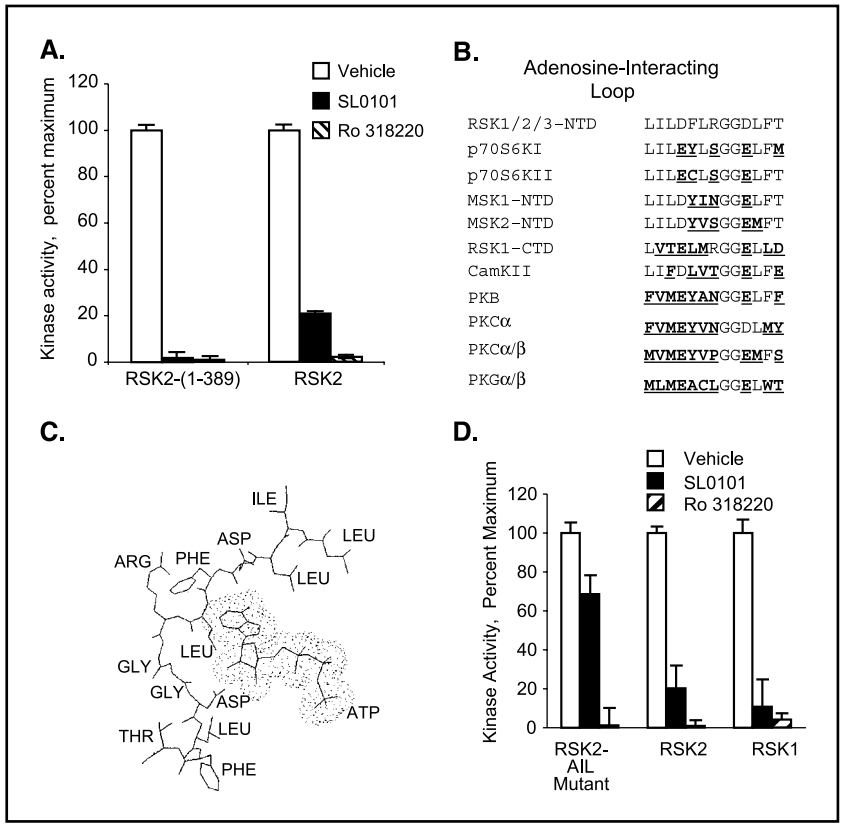

Figure 4. SL0101 inhibits activity of the NTKD. *A,* SL0101 inhibits activity of a RSK2 mutant lacking the CTKD. Hemagglutinin-tagged RSK2 and hemagglutinin-tagged truncation mutant containing the NTKD [RSK2 (1-389)] were transfected into baby hamster kidney 21 cells. Hemagglutinin-tagged proteins were immunoprecipitated from lysates of epidermal growth factor–stimulated cells. Assays were done as described in Fig. 1*A* in the presence of vehicle, 2 μmol/L SL0101, or 2 μmol/L Ro 318220. *Columns,* mean (n = 3 in triplicate); *bars,* SD. *B,* alignment of the primary structure of the AIL from several AGC kinase family members. *Asterisks,* residues in the AIL of RSK predicted to contact ATP based on the crystal structure of PKA; *underlined letters,* residues of the other AGC kinase family members differing from those of RSK. *C,* RSK NTKD AIL is modeled from the crystal structure of PKA. Amino acids are labeled and presented in *stick format*, whereas ATP is presented in *space-filling format*. *D,* RSK NTKD AIL is a major determinant for inhibition by SL0101. Hemagglutinin-tagged proteins were immunoprecipitated from the lysates of epidermal growth factor–stimulated baby hamster kidney 21 cells transfected with the indicated hemagglutinin-tagged constructs. Assays were done as described in Fig. 1*A* in the presence of vehicle, 2 μmol/L SL0101, or 2 μmol/L Ro 318220. *Columns,* mean (n = 3 in triplicate); *bars,* SD.

and S phases. This was also observed for U0126-treated MCF-7 cells (Fig. 6*D*), in agreement with published reports (22). It has been shown that activation of the MAPK pathway is required for the cells to reenter the cell cycle (23). Because SL0101 does not inhibit MAPK activity in intact cells, our data indicate that MAPK activity is not sufficient to initiate reentry into the cell cycle in these cells and that RSK activity is required to pass the G_1 restriction point.

We were able to substantially reduce RSK1 and RSK2 levels using siRNA (Fig. 7*A* and *B*). The data indicate that both RSK1 and RSK2 participate in MCF-7 cell proliferation. Interfering with RSK1 or RSK2 mRNA resulted in a proliferation rate that was 62% and 47% that of cells transfected with control siRNA, respectively. These results strongly support our observations that the RSKs are necessary for MCF-7 proliferation.

As further support of the specificity of SL0101 action, the proliferation of MCF-7 and MCF-10A cells was examined in the presence of other cell-permeable kinase inhibitors (Table 1; Supplemental Fig. 2). Kaempferol, the flavonoid constituent of

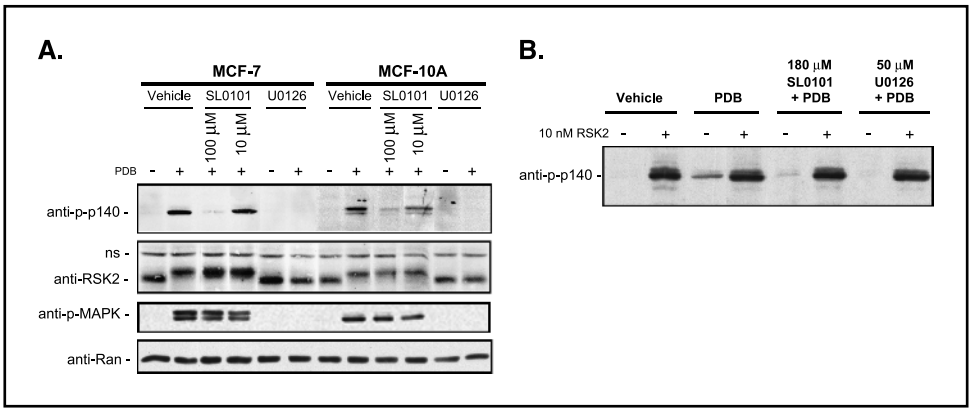

Figure 5. SL0101 is effective in intact cells. *A,* SL0101 inhibits phosphorylation of a RSK substrate in intact cells. MCF-7 and MCF-10A cells were preincubated with vehicle, 50 μmol/L U0126, or the indicated concentration of SL0101 for 3 hours. Cells were treated with 500 nmol/L PDB for 30 minutes before lysis. Protein concentration of lysates was measured, and lysates were electrophoresed, transferred, and immunoblotted. Equal loading of lysate is shown by the anti-Ran immunoblot. *B,* RSK directly phosphorylates pp140 *in vitro*. Serum-starved MCF-7 cells treated with vehicle, SL0101, or U0126 were stimulated with PDB or vehicle. Lysates were subjected to SDS-PAGE and transferred to nitrocellulose in preparation for immunoblotting. The nitrocellulose was cut into strips and incubated in the presence of kinase buffer or kinase buffer containing 10 nmol/L active RSK2. After extensive washing, the strips were placed in a single vessel for immunoblotting.

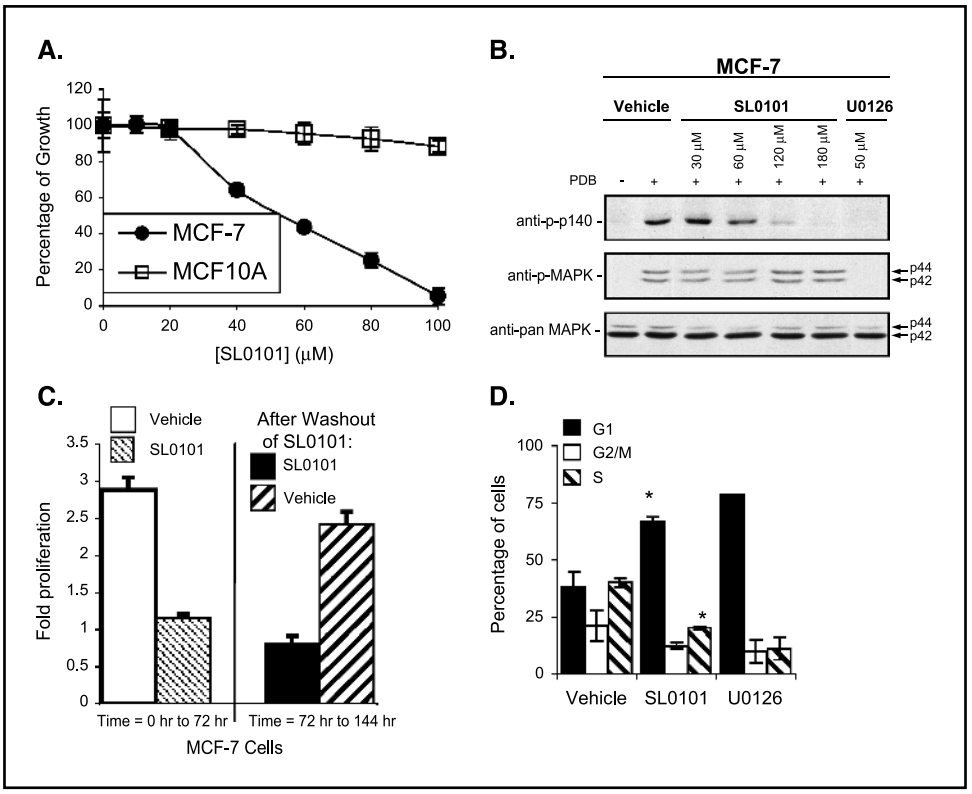

Figure 6. Effect of SL0101 on cell proliferation. *A,* SL0101 selectively inhibits MCF-7 cell proliferation. MCF-7 and MCF-10A cells were treated with vehicle or indicated concentration of SL0101, and cell viability was measured after 48 hours of treatment. Values are fold proliferation as a percentage of that observed with vehicle-treated cells. *Points,* mean (n = 3 in quadruplicate); *bars,* SD. *B,* inhibition of RSK activity by SL0101 parallels its effect on MCF-7 cell proliferation. Serum-starved MCF-7 cells were preincubated with vehicle, 50 μmol/L U0126, or the indicated concentration of SL0101 for 3 hours. Cells were treated with 500 nmol/L PDB for 30 minutes before lysis. Protein concentration of lysates was measured, and lysates were electrophoresed, transferred, and immunoblotted. Equal loading of lysate is shown by the anti-pan-MAPK immunoblot. *C,* MCF-7 cells resume normal growth after removal of SL0101. MCF-7 cells were treated with vehicle or 100 μmol/L SL0101. After 72 hours, the medium was washed out and replaced. Cell viability was measured. In separate plates, cells that had been incubated previously with SL0101 were treated with either 100 μmol/L SL0101 or vehicle and incubated for 72 hours. Cell viability was measured. *Columns,* mean (n = 2 in triplicate); *bars,* SD. *D,* SL0101 causes a G_1-S block in the cell cycle. MCF-7 cells were treated for 24 hours with either vehicle, 100 μmol/L SL0101, or 25 μmol/L U0126 before staining with propidium iodide and flow cytometry analysis. *Columns,* (n = 3); *bars,* SD. *, P = 0.005, Student's t test.

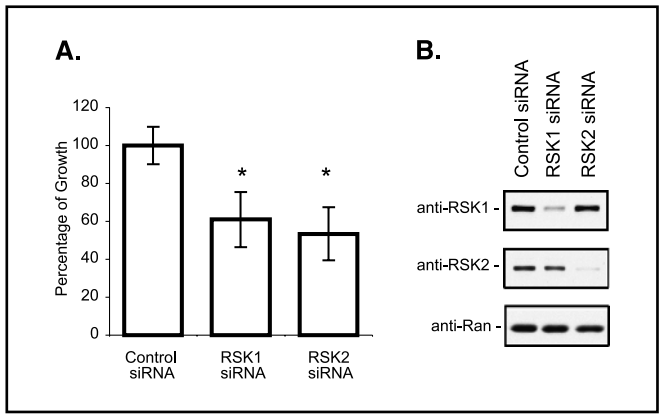

Figure 7. RNA silencing confirms that RSK is important for MCF-7 cell proliferation. *A,* reduction in RSK levels slows the growth of MCF-7 cells. Duplex nontargeting siRNA (*Control*) or RSK1- or RSK2-specific siRNA were transfected into MCF-7 cells. Cell viability was measured at 48 and 72 hours after transfection. Percentage of growth over the 24-hour period is depicted. Fold proliferation of the cells transfected with control siRNA is presented as 100%. *Columns,* mean (n = 2 of 12 replicates); *bars,* SD. *, $P \leq 0.0005$, compared with the control set (Student's t test). *B,* siRNAs reduce RSK protein levels. MCF-7 cells transfected as described in *A* were harvested 72 hours after transfection. Protein levels of RSK1 and RSK2 were examined by immunoblotting. Equal loading of lysate is shown by the anti-Ran immunoblot.

SL0101, slowed the growth of MCF-10A and MCF-7 cells to the same extent. U0126, the MAPK/ERK kinase inhibitor, halted proliferation of both MCF-7 and MCF-10A cells and therefore did not preferentially inhibit growth of the cancer cells. Ro 318220, a potent but nonspecific PKC inhibitor, which inhibits RSK as well as several other AGC kinase family members, also attenuated proliferation of both MCF-7 and MCF-10A cells to the same extent. The PKA inhibitor H89 was more effective at inhibiting the growth of the MCF-7 cells relative to that of the MCF-10A cells. However, concentrations of H89 that inhibited MCF-7 cell growth by ~80% also inhibited the growth of MCF-10A cells by ~40%. Therefore, unlike the action of these other kinase inhibitors, SL0101 selectively inhibits proliferation of the breast cancer cells without affecting the growth of the normal breast cells.

We also compared the phosphorylation patterns from MCF-7 cells preincubated with SL0101 to those from cells pretreated with other cell-permeable kinase inhibitors before stimulation with either PDB or a cocktail of I-E-F. The lysates were immunoblotted with multiple phosphospecific antibodies. As seen in Table 2 and Supplemental Fig. 3, concentrations of SL0101, Kaempferol, U0126, Ro 318220, and H89 that completely inhibit the growth of MCF-7 cells also inhibit phosphorylation of p140. However, all inhibitors,

Table 1. Proliferation of MCF-7 and MCF-10A cells in the presence of commercially available kinase inhibitors

	MCF-7 cells	MCF-10A cells
Kaempferol (μmol/L)		
50	87.6 ± 3.3	93.5 ± 3.7
100	32.3 ± 3.5	45.6 ± 1.6
250	6.1 ± 6.1	0 ± 0.3
U0126 (μmol/L)		
4	83.6 ± 6.3	60.7 ± 3.1
20	43.5 ± 3.5	18.7 ± 1.6
50	−4.5 ± 4.7	5.7 ± 2.6
Ro 318220 (μmol/L)		
0.25	83 ± 0.6	88.2 ± 2.4
0.5	56 ± 2.9	61.5 ± 3.2
1	−31 ± 4	−7 ± 1.3
H89 (μmol/L)		
2	71.2 ± 4.6	96.5 ± 2.2
4	21.5 ± 3	63.9 ± 5.5
8	−62.7 ± 1.7	20.4 ± 0.8

NOTE: MCF-7 and MCF-10A cells in the presence of 10% FCS were treated with vehicle or indicated concentration of compound. Cell viability was measured after 48 hours of treatment. Values given are the fold proliferation as a percentage of that observed with vehicle-treated cells. Negative values indicate that there were fewer viable cells after the 48-hour treatment than at the time treatment was initiated (time = 0 hour). The graphs from which this table was generated are included in Supplemental Fig. 2.

with the exception of SL0101, affected multiple phosphorylation events (Table 2; Supplemental Fig. 3). Whereas SL0101 only altered p140 phosphorylation. These data show that SL0101 does not inhibit PKA, PKC, Akt, or p70 S6K in intact cells. Additionally, SL0101 does not alter the profile of tyrosine phosphorylation in intact cells. Thus, with respect to these commercial kinase inhibitors, SL0101 shows specificity for RSK in intact cells. Interestingly, concentrations of each compound that halt MCF-7 cell growth also inhibit p140 phosphorylation, which suggests that p140 phosphorylation may be linked to proliferation in breast cancer cells.

It has been proposed that among the numerous events involved in tumorigenesis is an increased reliance on the compromised signaling pathway as well as the dormancy of alternative signaling pathways (24, 25). Thus, it seems that MCF-7 cells have become dependent on the RSK pathway, rendering the proliferation of these cells susceptible to inhibition by SL0101. The growth of MCF-10A cells would not be inhibited by SL0101 because intact signaling pathways provide numerous mechanisms for circumventing inhibition of a single signaling event. The involvement of RSK in breast cancer has not been examined previously. Interestingly, we have found that the mean levels of RSK1 and RSK2 in the cancer tissues are statistically higher than that in the normal tissues ($P < 0.05$, Student's t test). As shown by the box-and-whisker plots, ~50% of the cancer tissues displayed RSK1 or RSK2 levels significantly higher than the majority of the normal tissues. (Fig. 8*A*). Analysis of the RSK levels in the breast cancer tissue samples indicates that there is a positive linear relationship between RSK1 and RSK2 levels ($P = 0.0005$; data not shown), suggesting that regulation of both isozyme expression levels has become compromised. However, analysis of active MAPK levels indicates that all cancer tissue samples contained active MAPK, but there is no linear correlation between detectable active MAPK levels and RSK1 or RSK2 expression in the breast cancer tissues (Fig. 8*B*). Thus, the increase in RSK levels is not merely a reflection of overexpression of the various members of the MAPK pathway. We speculate that the growth of tumors, such as breast cancer, will be susceptible to inhibition by SL0101 and that RSK-specific

Table 2. Effect of SL0101 and commercially available kinase inhibitors on phosphorylation patterns in intact cells

Inhibitor	SL0101 (100 μmol/L)	H89 (8 μmol/L)	Kaempferol (250 μmol/L)	Ro318220 (1 μmol/L)	U0126 (50 μmol/L)
Stimulus	PDB/I-E-F	PDB/I-E-F	PDB/I-E-F	PDB/I-E-F	PDB/I-E-F
Phosphoprotein-specific antibodies					
p140	Inh/Inh	Inh/Inh	Inh/Inh	Inh/Inh	Inh/Inh
Ribosomal protein S6	NE/NE	Inh/NE	NE/Inh	Inh/NE	Inh/NE
CREB/activating transcription factor-1	NE/NE	Inh/NE	NE/NE	Inh/NE	Inh/NE
ERK	NE/NE	Inh/NE	NE/Inh	Inh/NE	Inh/Inh
Phospho-motif-specific antibodies					
PKA	NE/NE	Inh/NE	Stim/Stim	Inh/NE	Inh/NE
PKC	NE/NE	Inh/Inh	NE/Inh	Inh/Inh	NE/NE
Akt	NE/NE	Inh/Inh	Stim-Inh/Stim	Inh/Inh	Inh/NE
Phosphotyrosine	NE/NE	NE/NE	NE/Inh	NE/Inh	NE/NE

NOTE: Serum-starved MCF-7 cells were preincubated with vehicle or the indicated concentration of compound for 3 hours. Cells were treated with 500 nmol/L PDB or a cocktail of I-E-F for 30 minutes before lysis. Protein concentration of lysates was measured, and lysates were electrophoresed, transferred, and immunoblotted. Equal loading of lysate was shown by the anti-pan-MAPK immunoblot. Whether the compound altered the protein phosphorylation pattern compared with that observed with vehicle-treated cells is indicated by "Inh" for inhibition, "Stim" for stimulation of protein phosphorylation, or "NE" for no effect on the phosphorylation patterns. The immunoblots from which this table was generated are included in Supplemental Fig. 3.

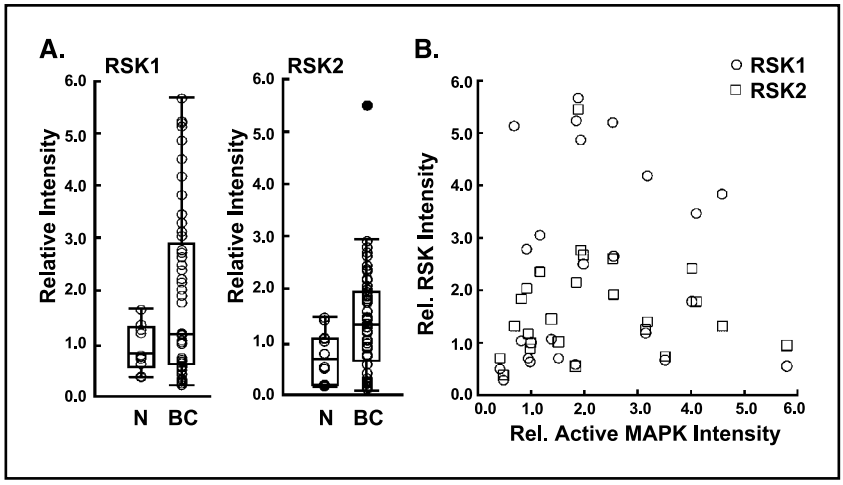

Figure 8. RSK is overexpressed in human breast cancer. Twelve normal (*N*) and 48 cancerous (*BC*; consisting of ductal and lobular carcinoma) breast tissue samples were ground under liquid nitrogen and lysed in SDS loading buffer. Normalized samples were then electrophoresed and immunoblotted with anti-RSK1, anti-RSK2, and anti-active MAPK antibodies. Immunoblots were analyzed by densitometry, and the intensities of RSK (*A*) were plotted as box-and-whisker plots according to Tukey (26). *Bar in the box,* statistical median; *ends of the box,* upper and lower quartiles. *Solid circle in the RSK2 plot,* statistical outlier and not included in the SD. Box-and-whisker plots clearly illustrate the range of the data. Mean of RSK1 and RSK2 levels in the cancer tissue samples and mean in the normal tissue samples are statistically different. $P \leq 0.05$ (Student's *t* test, two-tailed distribution). *B,* active MAPK levels were plotted against RSK1 and RSK2 protein levels measured in the breast cancer tissue. Statistical analysis of active MAPK and RSK levels generates a correlation coefficient that fails to be significant at $P \leq 0.05$; therefore, there is no linear correlation between active MAPK and RSK1 or RSK2 levels.

inhibitors, such as SL0101, may find widespread use as chemotherapeutic agents.

Our studies have uncovered an unexpected link between RSK activity and tumor cell proliferation revealing the value of RSK as a novel drug target. Additionally, we have identified the first RSK-specific inhibitor, SL0101, which will provide a powerful new tool for analyzing RSK function in a variety of biological systems. Additionally, this phytochemical is selectively cytostatic for a human breast cancer cell line without affecting the growth of a normal breast cell line. Thus, RSK-specific inhibitors may be useful as compounds for cancer chemotherapy.

Acknowledgments

Received 5/27/2004; revised 10/19/2004; accepted 11/19/2004.

Grant support: American Chemical Society, Virginia Chapter grant IRG 81-011-17, National Cancer Institute grant CA95335, and Department of Defense grant DAMD17-03-1-0366 USAMRMC.

The costs of publication of this article were defrayed in part by the payment of page charges. This article must therefore be hereby marked advertisement in accordance with 18 U.S.C. Section 1734 solely to indicate this fact.

We thank David L. Brautigan for establishing the infrastructure necessary for the drug discovery program; Ian G. Macara for his invaluable contributions during the research; Gregory P. Riddick for statistical analysis of the human tissue data; J. Thomas Parsons, Ian G. Macara, and Sarah J. Parsons for critical review of the article; and Michael J. Weber for discussions.

References

1. Jones SW, Erikson E, Blenis J, Maller JL, Erikson RL. A *Xenopus* ribosomal S6 kinase has two apparent kinase domains that are each similar to distinct protein kinases. Proc Natl Acad Sci U S A 1988;85:3377–81.
2. Dalby KN, Morrice N, Caudwell FB, Avruch J, Cohen P. Identification of regulatory phosphorylation sites in mitogen-activated protein kinase (MAPK)-activated protein kinase-1a/p90rsk that are inducible by MAPK. J Biol Chem 1998;273:1496–505.
3. Bjorbaek C, Zhao Y, Moller DE. Divergent functional roles for p90rsk kinase domains. J Biol Chem 1995;270:18848–52.
4. Fisher TL, Blenis J. Evidence for two catalytically active kinase domains in pp90rsk. Mol Cell Biol 1996;16:1212–9.
5. Jensen CJ, Buch MB, Krag TO, Hemmings BA, Gammeltoft S, Frodin M. 90-kDa ribosomal S6 kinase is phosphorylated and activated by 3-phosphoinositide-dependent protein kinase-1. J Biol Chem 1999;274:27168–76.
6. Poteet-Smith CE, Smith JA, Lannigan DA, Freed TA, Sturgill TW. Generation of constitutively active p90 ribosomal S6 kinase *in vivo*. Implications for the mitogen-activated protein kinase-activated protein kinase family. J Biol Chem 1999;274:22135–8.
7. Smith JA, Poteet-Smith CE, Malarkey K, Sturgill TW. Identification of an extracellular signal-regulated kinase (ERK) docking site in ribosomal S6 kinase, a sequence critical for activation by ERK *in vivo*. J Biol Chem 1999;274:2893–8.
8. Gavin AC, Nebreda AR. A MAP kinase docking site is required for phosphorylation and activation of p90(rsk)/MAPKAP kinase-1. Curr Biol 1999;9:281–4.
9. Leighton IA, Dalby KN, Caudwell FB, Cohen PT, Cohen P. Comparison of the specificities of p70 S6 kinase and MAPKAP kinase-1 identifies a relatively specific substrate for p70 S6 kinase: the N-terminal kinase domain of MAPKAP kinase-1 is essential for peptide phosphorylation. FEBS Lett 1995;375:289–93.
10. De Cesare D, Jacquot S, Hanauer A, Sassone-Corsi P. Rsk-2 activity is necessary for epidermal growth factor-induced phosphorylation of CREB protein and transcription of c-*fos* gene. Proc Natl Acad Sci U S A 1998;95:12202–7.
11. Ghoda L, Lin X, Greene WC. The 90-kDa ribosomal S6 kinase (pp90rsk) phosphorylates the N-terminal regulatory domain of IκBα and stimulates its degradation *in vitro*. J Biol Chem 1997;272:21281–8.
12. Joel PB, Traish AM, Lannigan DA. Estradiol-induced phosphorylation of serine 118 in the estrogen receptor is independent of p42/p44 mitogen-activated protein kinase. J Biol Chem 1998;273:13317–23.
13. Schouten GJ, Vertegaal AC, Whiteside ST, et al. IκBα is a target for the mitogen-activated 90 kDa ribosomal S6 kinase. EMBO J 1997;16:3133–44.
14. Xing J, Ginty DD, Greenberg ME. Coupling of the RAS-MAPK pathway to gene activation by RSK2, a growth factor-regulated CREB kinase. Science 1996;273:959–63.
15. Sutherland C, Leighton IA, Cohen P. Inactivation of glycogen synthase kinase-3β by phosphorylation: new kinase connections in insulin and growth-factor signalling. Biochem J 1993;296:15–9.
16. MSchwab MS, Roberts BT, Gross SD, et al. Bub1 is activated by the protein kinase p90(Rsk) during *Xenopus* oocyte maturation. Curr Biol 2001;11:141–50.
17. Palmer P, Gavin AC, Nebreda AR. A link between MAP kinase and p34(cdc2)/cyclin B during oocyte maturation: p90(rsk) phosphorylates and inactivates the p34(cdc2) inhibitory kinase Myt1. EMBO J 1998;17:5037–47.
18. Hemmer W, McGlone M, Taylor SS. Recombinant strategies for rapid purification of catalytic subunits of cAMP-dependent protein kinase. Anal Biochem 1997;245:115–22.
19. Zhang J, Chung TDY, Oldenburg KR. A simple statistical parameter for use in evaluation and validation of high throughput screening assays. J Biomol Screen 1999;4:67–73.
20. Matthes HWD, Luu B, Ourisson G. Cytotoxic components of *Zingiber zerumbet*, *Curcuma zedoaria* and *C. domestica*. Phytochemisty 1980;19:2643–50.
21. Sebolt-Leopold JS. Development of anticancer drugs targeting the MAP kinase pathway. Oncogene 2000;19:6594–5.
22. Lobenhofer EK, Huper G, Iglehart JD, Marks JR. Inhibition of mitogen-activated protein kinase and phosphatidylinositol 3-kinase activity in MCF-7 cells prevents estrogen-induced mitogenesis. Cell Growth 2000;11:99–110.
23. Pages G, Lenormand P, L'Allemain G, Chambard JC, Meloche S, Pouyssegur J. Mitogen-activated protein kinases p42mapk and p44mapk are required for fibroblast proliferation. Proc Natl Acad Sci U S A 1993;90:8319–23.
24. Mills GB, Lu Y, Kohn EC. Linking molecular therapeutics to molecular diagnostics: inhibition of the FRAP/RAFT/TOR component of the PI3K pathway preferentially blocks PTEN mutant cells *in vitro* and *in vivo*. Proc Natl Acad Sci U S A 2001;98:10031–3.
25. Neshat MS, Mellinghoff IK, Tran C, et al. Enhanced sensitivity of PTEN-deficient tumors to inhibition of FRAP/mTOR. Proc Natl Acad Sci U S A 2001;98:10314–9.
26. Tukey JW. Explanatory data analysis. Reading (MA): Addison-Wesley; 1977.